Marine Pollution Bulletin 128 (2018) 361–368

Contents lists available at ScienceDirect

Marine Pollution Bulletin

journal homepage: www.elsevier.com/locate/marpolbul

Baseline

Spatial and vertical distribution of radiocesium in seawater of the East China Sea

Lijun Zhao[a], Dantong Liu[a], Jinlong Wang[a,*], Jinzhou Du[a], Xiaolin Hou[b], Yifei Jiang[a]

[a] State Key Laboratory of Estuarine and Coastal Research, East China Normal University, Shanghai 200062, China
[b] Xi'an AMS Center and KLLQG, Institute of Earth Environment, Chinese Academy of Science, Xi'an 710075, China

ARTICLE INFO

Keywords:
^{137}Cs
Vertical profile
Spatial distribution
Seawater
East China Sea

ABSTRACT

The ^{137}Cs activity in surface water of the East China Sea (ECS) was 0.66–1.36 Bq m^{-3} during May of 2011. The low activities were observed in the Changjiang Estuary and Zhejiang-Fujian coast and high activities were observed in the south offshore and Kuroshio Current pathway, suggesting that the influence from the current system in the ECS. The ^{134}Cs were undetectable (< 0.03 Bq m^{-3}) and the contribution of the Fukushima accident to ECS is estimated to be below 3%; hence it is negligible during the investigation period. Using the vertical profiles of ^{137}Cs in the ECS, the mass balance is obtained, which suggests that the oceanic input dominates the ^{137}Cs source in the ECS. ^{137}Cs is potentially useful to trace water mass movement in the ECS. Our study provides comprehensive baseline of ^{137}Cs in the ECS for evaluation of the possible influence of the nuclear power plants in the future.

Radiocesium (^{134}Cs and ^{137}Cs) is derived from nuclear explosions since the world's first atomic bomb explosion in 1945, nuclear accidents, nuclear reprocessing facilities and nuclear power plants. The thermonuclear bomb testing mainly contributed to the global fallout ^{137}Cs (~900 PBq) (Hu et al., 2010). The nuclear accidents also released a bunch of ^{137}Cs to the earth environments (e.g., 85 PBq for Chernobyl) (UNSCEAR, 2008). Most recently, the accident happened in the Fukushima Dai-ichi Nuclear Power Plant (FDNPP) has released large amount of ^{137}Cs to the atmosphere (12 PBq) (Steinhauser et al., 2014). ^{137}Cs entered into the stratosphere was finally deposited on the earth globally, while those entered troposphere mainly distribute locally. Aarkrog (2003) estimated that around 603 PBq ^{137}Cs was input to ocean since 2000. Thus, ^{137}Cs is used for monitoring the nuclear contaminant around the nuclear reprocessing facilities and nuclear power plants (NPPs). The FDNPP derived radionuclides have dispersed and deposited almost all over the north hemisphere (Buesseler, 2012; Wang et al., 2012; Evrard et al., 2015). Among them, substantial fraction of them deposited to the ocean (Buesseler et al., 2012; Inoue et al., 2012; Suzuki et al., 2013). Investigations have shown the significantly increased level of ^{134}Cs and ^{137}Cs in the seawater samples in the offshore of Fukushima, as well as a large area in the Northwest Pacific Ocean (Honda et al., 2012; Povinec et al., 2013; Tumey et al., 2013).

Due to the relative conservative feature of ^{137}Cs in the ocean (Hirose et al., 1992), it has being utilized to trace the water mass and currents, and is useful to inspect and modify the ocean circulation model (Garraffo et al., 2016). East China Sea (ECS) is a broad and flat-continental shelf marginal sea of the Northwest Pacific. The complex current system and high concentration of suspended particles makes the ECS one of most important “sinks” of radionuclides and nutrients transported from the Northwest Pacific (Wang et al., 2017b). Besides, the surface of this area indicates a signature of “recirculated” seawater originates from intermediate layers of subtropical North Pacific (Miyazawa et al., 2009). However, the observation of ^{137}Cs around the ECS after accident was very limited. Wu et al. (2013) reported that the seawater ^{137}Cs was 1.08 ± 0.09 Bq m^{-3} in a few seawater samples (n = 8) and they suggest that FDNPP's accident might significantly enhance the ^{137}Cs level in the ECS, however, this database is too limited to assess the influence of FDNPP's accident associated with the transport of ^{137}Cs with water mass in the ECS. Wang et al. (2012) reported that ^{137}Cs activity in aerosols in Shanghai (about 50 km of the coast in the ECS) during 28th–29th March 2011 was 0.12 ± 0.09 mBq m^{-3}, which is significantly higher than the background level (0.04 mBq m^{-3}) before accident. These results urge a comprehensive observation of spatial and vertical distribution of ^{137}Cs in the ECS.

This work aims to investigate the level, distribution and source of radioactive cesium (^{134}Cs and ^{137}Cs) in the ECS by analyzing surface and profile seawater samples collected in the ECS during June 2011 in order to explore the impact of Fukushima accident in the ECS. Meanwhile, it can be also used to trace pathway of different water masses, and to supply a baseline for monitor the potential risk from 14

* Corresponding author.
E-mail address: jlwang@sklec.ecnu.edu.cn (J. Wang).

https://doi.org/10.1016/j.marpolbul.2018.01.047
Received 23 November 2017; Received in revised form 15 January 2018; Accepted 22 January 2018

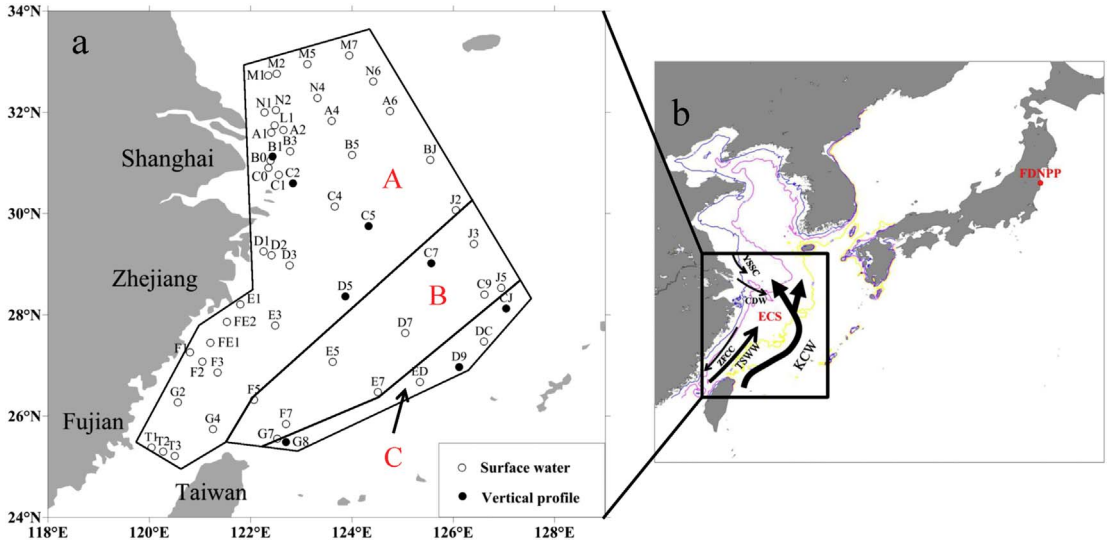

Fig. 1. (a) Sampling stations and water masses in the Changjiang Estuary and adjacent seas, solid circles represent vertical profile stations and hollow circles represent surface water stations, (b) Geographical thumbnail of water masses from the East China Sea (ECS) and the Fukushima Dai-ichi Nuclear Power Plant (FDNPP). Changjiang Diluted Water (CDW, summer), Taiwan Strait Warm Water (TSWW), Kuroshio Current Water (KCW) and Yellow Sea Surface Current (YSSC, summer) (modified from Su and Huh, 2002; Huang et al., 2013). The study area is divided into three parts, A: the water depth below 100 m, B: the water depth between 100 m and 1000 m, C: the water depth over 1000 m.

operating NPPs (as of May 2011) along the Chinese coast in the ECS as well as from the other nuclear facilities, nuclear accidents and other sources (e.g., oceanic input).

The ECS is a typical marginal sea and locates in the west of the Northwest Pacific Ocean (Fig. 1), receiving large amount of fresh water and sediment discharge from the Changjiang (Yangtze River), which is the largest river over the Euro-Asia continent (Dai et al., 2014). The ECS could be divided into the shallow western continental shelf and deep eastern continental shelf on the basis of the terrain of northwest high, southeast low. ECS owns complex water masses that interact with each other, such as the Changjiang Diluted Water (CDW), which extends at first along the estuary to the southeast until 122.50°E and then turns southward to form a tongue of diluted water in winter. The Zhejiang-Fujian Coast Current (ZFCC) is strong in winter and relatively weak in spring. The Kuroshio Current Water (KCW), a major western boundary current along the outer edge of the continental shelf, carrying a lot of high temperature and high salt water. The northward Taiwan Strait Warm Water (TSWW), with its upper water formed by the mixing of Kuroshio Current Surface Water and the Taiwan Strait Water, is originating from Kuroshio Current Subsurface Water (KCSSW) east of Taiwan (Lee et al., 2001; Lie and Cho, 2002; Lee and Chao, 2003; Lee and Takeshi, 2007). In the north part of the ECS shelf, the Yellow Sea Surface Current (YSSC) also participates in the structure of the ECS water masses (Su, 2001).

Seawater samples, including 55 surface seawater samples and 8 water profiles, were collected from 55 stations in the ECS (Fig. 1a) during the R/V "Shiyan 3" cruise between 11th May and 5th June 2011. An aliquot of 100 L seawater sample was collected from surface (0–0.5 m) and different depths of water columns by a submersible pump and a CTD rosette system, respectively. And then the samples were filtered by 0.5 μm pore-size pre-cleaned special polypropylene cartridge (Wang et al., 2017a).

Cesium in seawater sample was separated by adsorption using ammonium phosphomolybdate (AMP) at pH ~1.5 (Hirose et al., 2005; Yamada et al., 2006). Twenty five mg of CsCl was first spiked to 100 L seawater as the carrier and used for chemical yield tracer. The spiked seawater was stirred and equilibrated for 6 h. Forty grams AMP power (seawater) was added to each sample, the samples was then stirred for 30 min. After 24 h settlement the supernatant was siphoned out. The slurry with AMP/Cs precipitation was transferred to a 2 L plastic bottle and transported to the lab for further treatment. In the laboratory, the slurry was centrifuged to separate AMP-Cs precipitate, which was finally freeze-dried by a lyophilizer for radioactivity measurement.

Cesium-134 and Cesium-137 in the prepared samples were measured using a gamma spectrometer (GWL-120210-S, ORTEC) 604.7 keV (branch ratio = 97.6%) and 661.7 keV (branch ratio = 85.1%) gamma rays were used to calculate the concentration of ^{137}Cs and ^{134}Cs, respectively. The detection limits (LLD) of the gamma spectrometry system for both radionuclides were estimated to be 0.03 Bq m^{-3} for 100 L seawater. The chemical recoveries of about 78% for cesium were obtained by measuring of the stable Cs in the AMP precipitation after separation using atomic absorption spectrophotometer (America PE, AA-800). For analytical quality control, the IAEA standard source (IAEA-447) was analyzed for ^{137}Cs, the measurement results agreed with the certificated value.

The salinity and temperature in surface water of the ECS are plotted in Fig. 2. The temperature was 14.8–26.2 °C with a mean value of 20.1 °C, and the salinity was 24.2–34.6 with a mean value of 32.2. The temperature decreased from northwestern to southeastern and increased from the coast to offshore. The lowest temperature was observed in the north offshore of the ECS, and the highest value was observed in the south part of the ECS, especially in KCW pathway. The salinity increased from north to south and from west to east. The ^{137}Cs activities in all surface seawater samples from the ECS are shown in Table 1, and the range was 0.66–1.36 Bq m^{-3} with a mean value of 1.07 ± 0.09 Bq m^{-3} (n = 55). Lower ^{137}Cs activities were observed in the Changjiang Estuary, Zhejiang-Fujian coast and section C (from C0 to CJ) (Fig. 3). Higher values were observed in the northeast offshore and south offshore of the ECS (Fig. 3). Generally, the ^{137}Cs observed in this study is lower than the Yellow Sea (1.30–3.04 Bq m^{-3} with a mean value of 2.35 ± 0.44 Bq m^{-3}, Kim et al., 1997), Japan Sea (0.3–20.0 Bq m^{-3} with a mean value of 1.9 ± 0.1 Bq m^{-3}, Povinec et al., 2005) and the Western Pacific Ocean (0.5–23.7 Bq m^{-3} with a mean value of 1.8 ± 0.1 Bq m^{-3}, Povinec et al., 2005), and meanwhile is similar to the South China Sea (1.14–1.41 Bq m^{-3} with a mean value of 1.28 ± 0.08 Bq m^{-3}, Wu et al., 2013).

The ^{137}Cs in five vertical profiles (B1, C2, C5, C7 and D5) are slightly higher in bottom layer compared to the surface layer and generally showed the stable vertical distribution. These distribution patterns are similar with the profiles of temperature and salinity distribution (Fig. 4). This should be attributed to the sufficiently mixing derived by the complex current system. The vertical profiles of ^{137}Cs

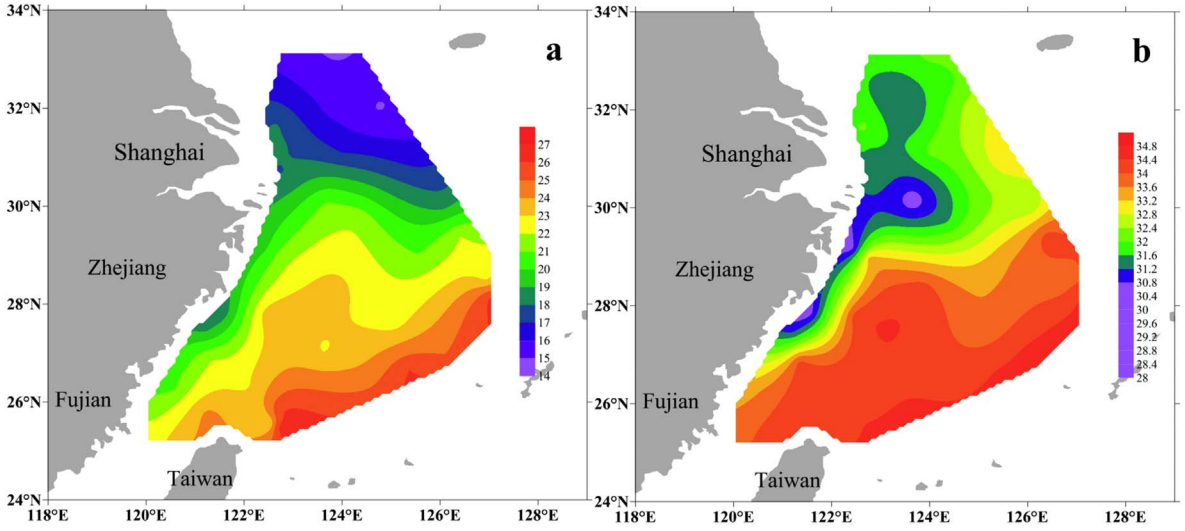

Fig. 2. Contour plots of temperature (°C) (a) and salinity (b) in surface water of the East China Sea.

activities at three deep-water stations (i.e., G8, D9 and CJ) are shown in Fig. 5. These three stations are located in the Okinawa trough with water depth of over 1000 m. The higher values were observed in the subsurface water of station CJ and D9 with a high salinity level (over 34.5). The maximum values were observed in the intermediate water of station G8, CJ and D9 with a salinity of 34.3–34.4. These high ^{137}Cs activities should be attributed to open seawater input from the strong KCSSW (Zhang et al., 2007; Qi et al., 2014). The ^{137}Cs activities at the bottom water of these three stations were lowest, to be 0.96 ± 0.09 Bq m^{-3} (1000 m at CJ), 0.76 ± 0.10 Bq m^{-3} (870 m at G8) and 0.35 ± 0.05 Bq m^{-3} (1000 m at D9), respectively. These values were comparable to those in previous investigations and could be considered as the background of ^{137}Cs in deep seawater in the West Pacific Ocean (Povinec et al., 2011).

^{137}Cs in the ECS water column potentially originated from Changjiang input, atmospheric fallout from global weapons testing, emission from the nuclear reprocessing plants, nuclear power plant accident and open sea input.

FDNPP accident has released large amount of ^{137}Cs to atmosphere and the east adjacent seas (Stohl et al., 2012; Smith et al., 2015). ^{137}Cs in coastal seawater along the Northern Sanriku and Tsugaru Strait in northeastern Japan during May and June of 2011 have been reported to be 1.9–3.9 Bq m^{-3} (mean: 2.74 Bq m^{-3}, n = 29) and this mean value is higher than the background level in coastal seawater of northeastern Japan before accident (Inoue et al., 2012) and three times higher than the result of our study. Similar level of ^{134}Cs were also detected to be 0.4–2.8 Bq m^{-3} (mean: 1.37 Bq m^{-3}, n = 29) in seawater samples from northeastern Japan, which suggest that the significant impact from the FDNPP (Inoue et al., 2012) in the seawater offshore Fukushima. However, ^{134}Cs in seawater of the ECS during May of 2011 was not measureable (< 0.03 Bq m^{-3}), this suggests that ^{137}Cs derived from Fukushima accident is less important in the ECS. The activity ratio of ^{134}Cs/^{137}Cs from the FDNPP accident was reported to be ~1 (http://www.mext.go.jp/english/incident/1303962.htm). Based on this ratio, the LLD (0.03 Bq m^{-3}) of ^{134}Cs, and the mean value of ^{137}Cs (1.07 ± 0.09 Bq m^{-3}, n = 55) in the ECS, it can be estimated that < 3% of ^{137}Cs in the ECS was attributed to the FDNPP. Based on one vertical profile station data with three water depths, Wu et al. (2013) suggested that the atmospheric fallout from the FDNPP significantly enhanced the ^{137}Cs level of the surface water in the ECS during May and June. The results of this comprehensive investigation do not support this conclusion, and suggests that Wu et al. (2013) overestimated the contribution of ^{137}Cs from Fukushima accident.

For the emission from the NPPs in the south China coasts, previous studies have reported that these contributions are ignorable for the ECS (Du et al., 2010; Liu et al., 2016; Wang et al., 2017b). The ^{137}Cs activity in coastal areas of the ECS which is near the NPPs was not observed to be significantly different or higher than that of neighboring waters and conversely, it was lower than other regions. This observation further confirms that contribution from the NPPs in the south China coast was ignorable for the ECS.

Though a number of nuclear weapons tests were conducted in the north hemisphere including those conducted in Northwest China and Kazakhstan (Matzko, 1994; Bauer et al., 2005), but these released ^{137}Cs was negligible for the ECS due to very long distance from the test sites to the ECS (> 2500 km). This is confirmed by measurement of sediment cores in the ECS, where no ^{137}Cs signals of these nuclear tests were detected in the sediment cores (Wang et al., 2016, 2017b). Chernobyl accidents has released large amount of radioactive substances to the environment including ^{137}Cs (Balonov, 2007; Izrael, 2007), but most of them were deposited in the Europe (De et al., 1998; Izrael, 2007). Although ^{137}Cs and ^{131}I signals of Chernobyl accident were measured in China, but it was mainly observed in North China, the deposition in the South China is negligible. The measurement of ^{137}Cs in sediment of the ECS and soil of south China coast did not show any significant signal of Chernobyl fallout (Du et al., 2010; Wu et al., 2010; Wang et al., 2016). In addition, the investigation of ^{129}I and Pu isotopes in the ECS did not found any significant contribution of Chernobyl fallout in this region (Liu et al., 2016; Wang et al., 2017b). Thus the contribution of Chernobyl accident fallout in the ECS was also negligible. However, previous studies have suggested that the long transport of oceanic artificial radionuclides contributed a lot to the ECS, such as Pu and ^{137}Cs (Du et al., 2010; Liu et al., 2011; Wang et al., 2017b). They suggested that the close-in fallout of artificial radionuclides can be transported into the ECS via the North Equatorial Current and the KCW.

Compared to the source terms discussed above, the riverine input and atmospheric fallout should be also important for the ^{137}Cs source in the ECS. Du et al. (2010) reported that the annual Changjiang input ^{137}Cs was (5.10 ± 3.06) × 10^{10} Bq y^{-1}, and other riverine contribution to the ECS was negligible. The data of atmospheric fallout ^{137}Cs is not available for the ECS, but the annual deposition fluxes of ^{137}Cs in a nearest city of Shanghai (31.23°N, 121.40°E) was estimated to be 0.33 ± 0.20 Bq m^{-2} y^{-1} (Du et al., 2010). Taking the surface area of this study region (3.00 × 10^5 km^2), the atmospheric fallout ^{137}Cs can be estimated to be (9.90 ± 3.96) × 10^{10} Bq y^{-1}. This value is slightly higher than the Changjiang input.

Therefore, it can be concluded that ^{137}Cs in the ECS water column mainly originated from Changjiang input, direct atmospheric fallout

Table 1
^{137}Cs activities of seawater in the East China Sea during 11th May to 5th June 2011.

Station	Latitude (°N)	Longitude (°E)	Water depth (m)	Sampling depth (m)	Temperature (°C)	Salinity	^{137}Cs (Bq m^{-3})
T3	25.21	120.50	78	0.5	23.4	34.1	1.19 ± 0.08
T2	25.30	120.27	58	0.5	22.2	33.9	1.00 ± 0.09
T1	25.38	120.05	60	0.5	22.5	34.0	1.03 ± 0.10
G2	26.27	120.57	67	0.5	20.9	33.6	1.08 ± 0.08
G4	25.74	121.25	80	0.5	24.3	34.2	1.16 ± 0.11
F7	25.84	122.70	111	0.5	25.8	34.1	1.00 ± 0.04
G8	25.48	122.70	1325	0.5	26.2	34.6	1.14 ± 0.10
G8	25.48	122.70	1325	50	25.6	34.8	0.91 ± 0.08
G8	25.48	122.70	1325	200	17.5	34.5	1.14 ± 0.07
G8	25.48	122.70	1325	400	11.3	34.4	1.12 ± 0.12
G8	25.48	122.70	1325	870	5.1	34.4	0.76 ± 0.10
G7	25.55	122.52	310	0.5	22.9	34.0	1.03 ± 0.11
F5	26.32	122.07	106	0.5	22.9	34.2	1.16 ± 0.14
F3	26.86	121.35	70	0.5	22.0	34.1	1.04 ± 0.06
F1	27.26	120.81	25	0.5	18.4	29.8	0.66 ± 0.10
FE1	27.45	121.21	30	0.5	18.9	31.2	0.93 ± 0.11
FE2	27.86	121.53	30	0.5	18.1	30.5	0.86 ± 0.05
E1	28.21	121.80	23	0.5	17.2	32.2	0.81 ± 0.07
E3	27.79	122.48	85	0.5	23.6	34.2	1.16 ± 0.11
E5	27.07	123.62	116	0.5	22.9	34.3	1.17 ± 0.07
E7	26.47	124.51	153	0.5	24.5	34.2	1.12 ± 0.10
ED	26.67	125.34	1066	0.5	26.0	34.4	1.12 ± 0.09
D9	26.97	126.12	1507	0.5	25.0	34.6	1.00 ± 0.08
D9	26.97	126.12	1507	30	24.9	34.6	1.36 ± 0.17
D9	26.97	126.12	1507	50	24.9	34.6	1.17 ± 0.07
D9	26.97	126.12	1507	160	21.8	34.7	0.97 ± 0.10
D9	26.97	126.12	1507	400	10.5	34.3	1.44 ± 0.07
D9	26.97	126.12	1507	1000	4.4	34.4	0.35 ± 0.05
DC	27.47	126.61	1588	0.5	25.4	34.5	1.11 ± 0.10
D7	27.64	125.05	102	0.5	22.5	33.6	0.94 ± 0.06
D5	28.36	123.87	80	0.5	23.3	34.2	1.07 ± 0.09
D5	28.36	123.87	80	36	21.7	34.3	1.20 ± 0.10
D5	28.36	123.87	80	50	21.2	34.3	1.30 ± 0.13
D5	28.36	123.87	80	76	19.0	34.5	1.33 ± 0.14
D3	28.98	122.77	63	0.5	21.5	33.3	1.10 ± 0.08
D1	29.25	122.25	17	0.5	18.1	31.7	1.11 ± 0.06
C2	30.60	122.83	40	0.5	18.0	31.5	1.05 ± 0.11
C2	30.60	122.83	40	36	16.9	33.7	1.51 ± 0.17
C4	30.14	123.66	67	0.5	20.9	30.5	0.81 ± 0.06
C5	29.75	124.33	76	0.5	21.7	31.5	1.06 ± 0.10
C5	29.75	124.33	76	34	17.3	34.0	1.03 ± 0.06
C5	29.75	124.33	76	50	17.2	34.0	1.09 ± 0.13
C5	29.75	124.33	76	73	17.2	34.0	1.54 ± 0.12
C7	29.02	125.57	105	0.5	21.0	33.5	0.93 ± 0.11
C7	29.02	125.57	105	28	18.1	34.1	1.31 ± 0.13
C7	29.02	125.57	105	45	18.0	34.5	1.22 ± 0.10
C7	29.02	125.57	105	70	17.5	34.5	1.48 ± 0.10
C9	28.40	126.61	159	0.5	23.6	33.8	0.85 ± 0.03
CJ	28.13	127.05	1027	0.5	26.2	34.4	1.00 ± 0.09
CJ	28.13	127.05	1027	30	24.5	34.7	1.05 ± 0.12
CJ	28.13	127.05	1027	50	24.6	34.8	1.64 ± 0.15
CJ	28.13	127.05	1027	100	23.8	34.8	1.33 ± 0.13
CJ	28.13	127.05	1027	280	14.0	34.5	1.84 ± 0.10
CJ	28.13	127.05	1027	1000	4.5	34.4	0.96 ± 0.09
J5	28.53	126.95	322	0.5	22.7	33.9	1.36 ± 0.11
J3	29.40	126.41	100	0.5	22.0	34.2	1.28 ± 0.08
J2	30.07	126.05	81	0.5	18.4	32.4	1.18 ± 0.10
BJ	31.06	125.55	65	0.5	16.4	33.2	1.13 ± 0.08
B5	31.16	124.00	50	0.5	16.8	32.1	1.00 ± 0.08
B3	31.23	122.78	50	0.5	18.1	31.6	1.08 ± 0.10
A1	31.60	122.41	24	0.5	17.1	29.9	1.15 ± 0.06
A2	31.65	122.65	34	0.5	18.1	32.1	0.98 ± 0.11
A4	31.83	123.60	40	0.5	16.1	31.3	1.11 ± 0.07
A6	32.02	124.75	45	0.5	14.9	32.5	1.21 ± 0.10
N6	32.61	124.42	49	0.5	15.7	31.9	1.14 ± 0.06
N4	32.28	123.32	39	0.5	16.0	31.2	1.12 ± 0.08
N2	32.04	122.50	28	0.5	16.6	31.6	1.32 ± 0.11
N1	32.00	122.28	21	0.5	17.0	31.4	0.74 ± 0.04
M1	32.72	122.35	25	0.5	15.6	24.6	1.23 ± 0.10
M2	32.76	122.51	28	0.5	15.4	31.8	1.33 ± 0.10
M5	32.95	123.12	32	0.5	15.4	31.7	0.97 ± 0.09
M7	33.13	123.95	56	0.5	14.8	32.1	1.01 ± 0.08
L1	31.74	122.47	26	0.5	17.4	31.6	1.18 ± 0.11

(*continued on next page*)

Table 1 (*continued*)

Station	Latitude (°N)	Longitude (°E)	Water depth (m)	Sampling depth (m)	Temperature (°C)	Salinity	^{137}Cs (Bq m^{-3})
B1	31.13	122.43	14	0.5	19.1	24.6	1.10 ± 0.12
B1	31.13	122.43	14	12	18.0	29.1	1.13 ± 0.08
B0	31.04	122.39	13	0.5	19.1	24.2	1.15 ± 0.09
C0	30.90	122.35	15	0.5	18.7	27.1	0.95 ± 0.10
C1	30.77	122.56	19	0.5	18.3	29.9	1.16 ± 0.11
D2	29.18	122.41	39	0.5	19.7	30.6	1.16 ± 0.07
F2	27.08	121.04	46	0.5	20.7	32.4	1.00 ± 0.04
Min					4.4	16.3	0.35 ± 0.05
Max					26.8	34.8	1.84 ± 0.10

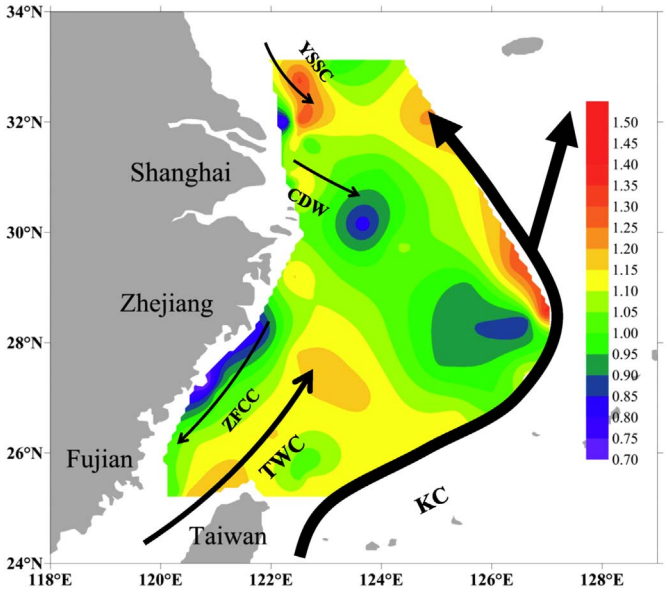

Fig. 3. The spatial distribution of ^{137}Cs activities (Bq m^{-3}) in surface water with the water masses of the East China Sea.

from global weapons testing and sea currents input.

Based on the vertical profiles of ^{137}Cs activities data, inventory of ^{137}Cs in each vertical profile (G8, D9 and CJ) can be estimated using follow equation (Aoyama and Hirose, 2003; Ito et al., 2003):

$$I = \frac{1}{2}\left\{\sum_{i=1}^{N}(C_{i+1}+C_i)(d_{i+1}-d_i) + 2C_1d_1 + 2C_N(d_B-d_N)\right\} \quad (1)$$

where N, C_i and d_i refer to the number of sampling depths, ^{137}Cs activity (Bq m^{-3}) in seawater at depth i and the ith sampling depth (m), respectively. In addition, d_1 and d_B represent the first sampling depth (m) and the total depth to the bottom (m), respectively.

The estimated inventory of ^{137}Cs (I) at stations G8, D9 and CJ were 1.22 ± 0.09, 1.18 ± 0.05 and 1.45 ± 0.09 kBq m^{-2}, respectively. A pre-FDNPP accident inventory of ^{137}Cs (CB-11, 25.24°N, 124.52°E) near station D9 has been previously reported to be 1.90 kBq m^{-2} (decay corrected to June of 2011; Nagaya and Nakamura, 1992), which is higher than that at D9 estimated in this study. This also confirmed that the contribution of the FDNPP accident derived ^{137}Cs in the ECS is insignificant.

The main sources of ^{137}Cs in the ECS water column include Changjiang input, atmospheric fallout from global weapons testing and sea currents input. While, ^{137}Cs in the water column was removed through deposition to the bottom sediment, flowed out to adjacent seas and the radioactive decay. The input and output of ^{137}Cs to the adjacent seas is combined to a net source or sink item which would be estimated later. Assumed a steady state of ^{137}Cs in the ECS water column, the ^{137}Cs mass balance in the water column of this region can be evaluated.

The vertical distribution of ^{137}Cs in deep waters and shallow waters are different. In this study area, the shallow area A (with water depth below 100 m) (Fig. 1) accounts for 65% of the total area with the mean depth of 45 m, and the deep area B (water depth between 100 and 1000 m) (Fig. 1) accounts for 32% of the total area with the mean depth of 158 m. The total ^{137}Cs in deep water column can be calculated to be (1.18 ± 0.04) × 10^{13} Bq based on the inventory of ^{137}Cs (I) at stations of G8, D9 and CJ and the study area of 9.20 × 10^3 km^2. ^{137}Cs in shallow

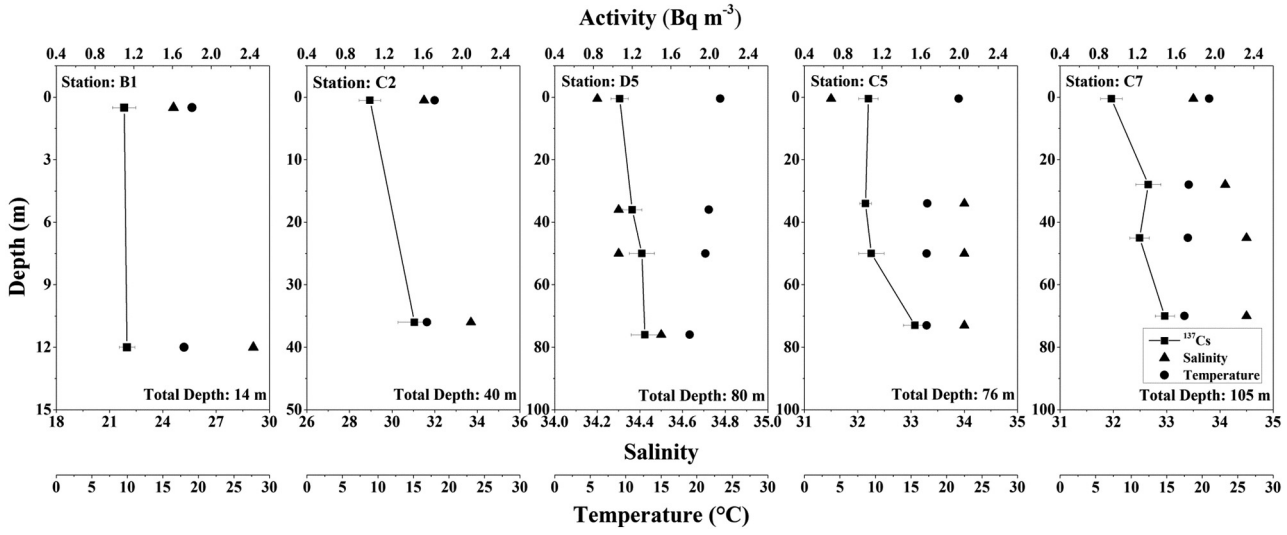

Fig. 4. Vertical profiles of ^{137}Cs activity (squares) at shallow column, temperature (circles) and salinity (triangles) at five typical stations in the ECS.

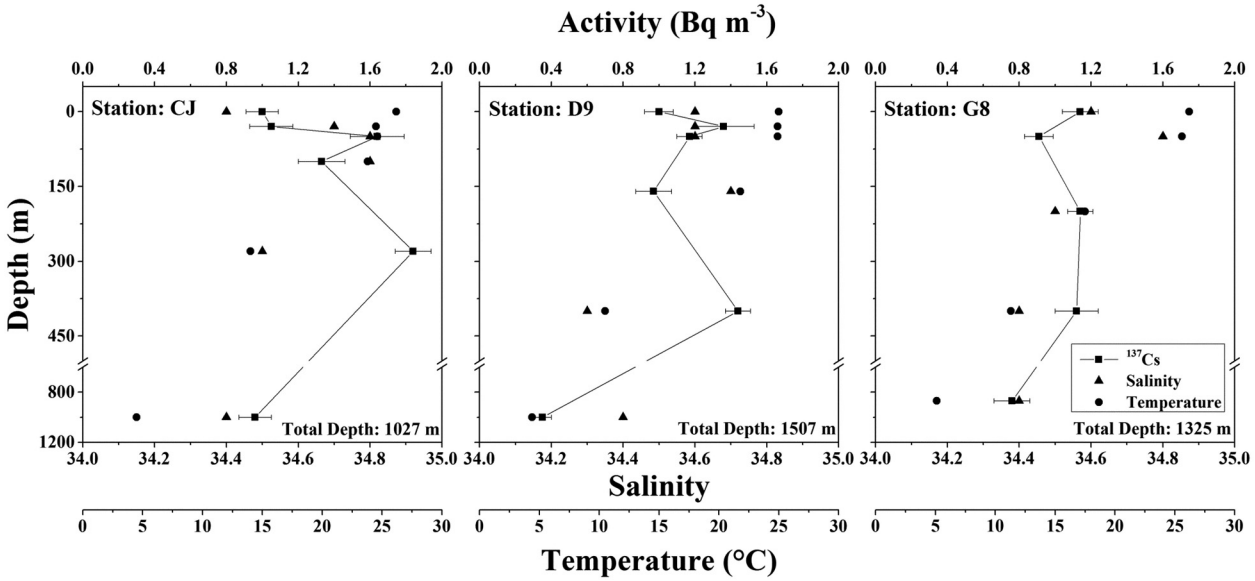

Fig. 5. Vertical profiles of ^{137}Cs activity (squares) at deep water column, temperature (circles) and salinity (triangles) at three typical stations in the ECS.

water is well-mixed, the total ^{137}Cs at these waters was estimated to be $(2.59 \pm 0.02) \times 10^{13}$ Bq by using the mean ^{137}Cs activities of 1.07 ± 0.01 Bq m^{-3} (n = 50, including the profile data) and the water volume 2.42×10^{13} m^3. Thus the total ^{137}Cs in the ECS is estimated to be $(8.65 \pm 0.10) \times 10^{11}$ Bq y^{-1} by using the sum values of shallow and deep waters ($(3.77 \pm 0.04) \times 10^{13}$ Bq) divided by the mean lifetime of ^{137}Cs (43.6 y). Among three sinks of ^{137}Cs in the ECS, the decay of ^{137}Cs during one year is 2.3% that is much smaller than the uncertainty associated with the mass balance and thus is omitted here. The ^{137}Cs buried in the sediment column of the ECS should be important sink and previous study suggest that the mean sedimentary flux of ^{137}Cs in the ECS sediment was (8.53 ± 1.71) Bq m^{-2} y^{-1} (Du et al., 2010). Using this data and the surface area of the ECS (3.00×10^5 km^2), we can estimate that the buried ^{137}Cs is $(2.56 \pm 0.51) \times 10^{12}$ Bq y^{-1}. The sum of riverine and atmospheric input ^{137}Cs is $(1.50 \pm 0.50) \times 10^{11}$ Bq y^{-1}, which is far less than the ^{137}Cs buried in the sediments and stored in the water column ($(3.42 \pm 0.01) \times 10^{12}$ Bq y^{-1}). The sea current input of ^{137}Cs can therefore estimated to be $(3.27 \pm 0.51) \times 10^{12}$ Bq y^{-1}, which is clearly a dominant source of ^{137}Cs in the ECS. Finally, the mass balance of ^{137}Cs is obtained as Fig. 6.

Based on the relative conservative feature of Cs in the ocean, ^{137}Cs has been widely used as oceanographic tracer for water circulation (Smith et al., 1998; Delfanti et al., 2003) and water mass interaction (Miyao et al., 2000), meanwhile it can be also used to monitor and evaluate the dispersion of releases from nuclear accident and nuclear facilities (Honda et al., 2012). Using the method proposed by Sholkovitz (1983), the apparent residence time of ^{137}Cs in the ECS can be estimated to be 15 y by using the water-column storage ^{137}Cs ($(3.77 \pm 0.04) \times 10^{13}$ Bq) divided by the sedimentary rate of ^{137}Cs ($(2.56 \pm 0.51) \times 10^{12}$ Bq y^{-1}). This relatively long residence time of ^{137}Cs in the ECS water column suggests that ^{137}Cs is potentially useful to trace the water mass movement in the ECS.

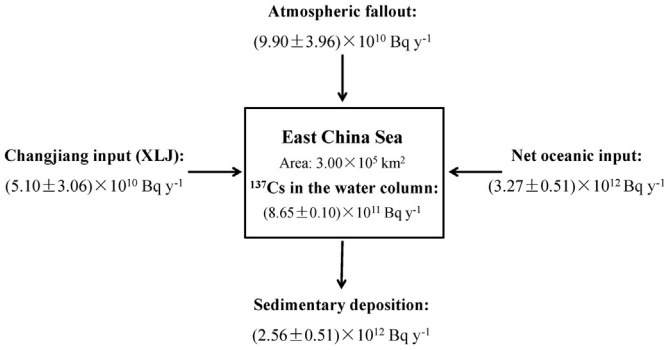

Fig. 6. Mass balances of ^{137}Cs in the ECS.

The main water masses in the ECS are reported to CDW, KCSSW, Kuroshio Current Surface Water (KCSW), Kuroshio Current Intermediate Water (KCIW), TSWW and part of YSSC in the ECS (Chen et al., 1995; Chen, 2009). And with some classification of the sampling stations, Table 2 summarized the variation ranges of salinity and temperature for each water mass. The ^{137}Cs activity is plotted in Fig. 7 associated with the T-S diagram. Besides, the distribution pattern of ^{137}Cs in surface water corresponds to the current system in the ECS (Fig. 3). Along the Changjiang Estuary, Zhejiang-Fujian coast and section C (Fig. 3), the ^{137}Cs activities also showed the low values. These trend might be attributed to the influence of the riverine fresh water, because the low level dissolved ^{137}Cs is usually observed in the river water due to its higher particle affinity (K_d: ~10^5 L kg^{-1}) (Wang et al., 2017a). Moreover, the low-^{137}Cs region is corresponding to the distribution pattern of the CDW and ZFCC in spring, which further suggests the significant role of these currents in ^{137}Cs distribution. The temperature and salinity in Changjiang Estuary and its southern coast also showed low values, which further suggest the influence of the CDW and ZFCC in spring. The lowest temperature was likely influenced by the YSSC. In the south offshore of the ECS, the ^{137}Cs showed higher values, which might be attributed to oceanic input of ^{137}Cs from the KCW and TWC (Su and Huh, 2002; Wang et al., 2017b). The temperature and salinity in this region were also higher. Previous investigations have shown that the ^{137}Cs in surface water of Northwest Pacific are much higher than those from the ECS (2–3 Bq m^{-3}, Povinec et al., 2003, 2005). The higher values of ^{137}Cs were also found in north offshore of the ECS, where a branch of the KCW, the YSWC, flows northwestward (Nagaya and Nakamura, 1992; Kim et al., 1997). Generally, ^{137}Cs activities were higher in more salty seawater, especially where the salinity was over 32, since high salinity could promote the desorption of ^{137}Cs from the particles (Smith et al., 1998; Hirose et al., 2007; Inoue et al., 2012). Considering relatively long residence time and oceanic dominate-source of ^{137}Cs in the ECS, ^{137}Cs is potentially utilized to trace the long-transport of the dissolved species from the oceanic input by the KCW and TWC.

Table 2
Classification of the sampling stations by temperature and salinity.

Water mass	Station	Temperature (°C)	Salinity	Reference
CDW	A2, A6, M1, B1, C0, F1, FE1, FE2, E1, D1, C2, C4, C5, B5, B3, A1, A4, N4, N2, N1, L1 B1-12, B0, C1, D2, F2	13.4–23.5	26.0–32.0	Chang and Isobe, 2003 Wang et al., 2012
KCSW	F7, G8, G8-50, E7, ED, D9, D9-30, D9-50, DC, CJ, CJ-30, CJ-50	19.0–27.8	34.3–34.8	
KCSSW	G8-200, D9-160, CJ-100	13.0–23.3	34.6–35.0	
KCIW	G8-400, D9-400, CJ-280	6.5–13.6	34.1–34.5	Qi et al., 2014
TSWW	T3, T2, T1, G2, G4, F5, F3, D5, D5-36, D5-50, D5-76	17.0–25.3	33.3–34.6	Takano, 1991
YSSC	M7	11.5–15.5	32.0–33.2	

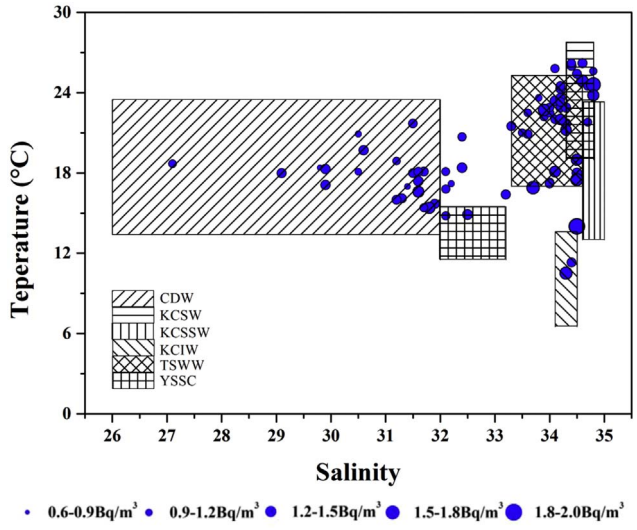

Fig. 7. T-S diagram for seawater samples with ^{137}Cs activities of the East China Sea in 2011. The temperature and salinity range of water mass in T-S diagram is plotted according to the previous study (Takano, 1991; Chang and Isobe, 2003; Wang et al., 2012; Qi et al., 2014).

Acknowledgments

This research was supported by the China Postdoctoral Science Foundation (2017M610238), National Natural Science Foundation of China (41706089), State Key Laboratory of Estuarine and Coastal Research (SKLEC-KF201602, SKLEC-KF201402), and Special Fund for Oceanic-scientific Research in the Public Interest (201505005-5).

References

Aarkrog, A., 2003. Input of anthropogenic radionuclides into the World Ocean. Deep-Sea Res. II Top. Stud. Oceanogr. 50 (17), 2597–2606.
Aoyama, M., Hirose, K., 2003. Temporal variation of ^{137}Cs water column inventory in the North Pacific since the 1960s. J. Environ. Radioact. 69, 107–117.
Balonov, M.I., 2007. The Chernobyl Forum: major findings and recommendations. J. Environ. Radioact. 96 (1), 6–12.
Bauer, S., Gusev, B.I., Pivina, L.M., Apsalikov, K.N., Grosche, B., 2005. Radiation exposure due to local fallout from Soviet atmospheric nuclear weapons testing in Kazakhstan: solid cancer mortality in the Semipalatinsk historical cohort, 1960–1999. Radiat. Res. 164 (4), 409–419.
Buesseler, K.O., 2012. Fishing for answers off Fukushima. Science 338 (6106), 480–482.
Buesseler, K.O., Jayneb, S.R., Fisher, N.S., Rypina, I.I., Baumann, H., Baumann, Z., Breier, C.F., Douglass, E.M., George, J., Macdonald, A.M., Miyamoto, H., Nishikawa, J., Pike, S.M., Yoshida, S., 2012. Fukushima-derived radionuclides in the ocean and biota off Japan. Proc. Natl. Acad. Sci. 109 (16), 5984–5988.
Chang, P., Isobe, A., 2003. A numerical study on the Changjiang diluted water in the Yellow and East China Seas. J. Geophys. Res. 108 (C9), 3299.
Chen, C.T.A., 2009. Chemical and physical fronts in the Bohai, Yellow and East China seas. J. Mar. Syst. 78 (3), 394–410.
Chen, C.T.A., Ruo, R., Paid, S.C., Liu, C.T., Wong, G.T.F., 1995. Exchange of water masses between the East China Sea and the Kuroshio off northeastern Taiwan. Cont. Shelf Res. 15 (1), 19–39.
Dai, Z.J., Liu, J.T., Wei, W., Chen, J.Y., 2014. Detection of the Three Gorges Dam influence on the Changjiang (Yangtze River) submerged delta. Sci. Rep. 4, 6600.
De, C.M., Dubois, G., Fridman, S.D., Germenchuk, M.G., Izrael, Y.A., Janssens, A., Jones, A.R., Kelly, G.N., Kvasnikova, E.V., Matveenko, I.I., Nazarov, I.M., Pokumeiko, Y.M., Sitak, V.A., Stukin, E.D., Tabachny, L.Y., Tsaturov, Y.S., Avdyushin, S.I., 1998. Atlas of Caesium Deposition in Europe After the Chernobyl Accident. European Commission, Luxemburg.
Delfanti, R., Klein, B., Papucci, C., 2003. Distribution of ^{137}Cs and other radioactive tracers in the eastern Mediterranean: relationship to the deepwater transient. J. Geophys. Res. Oceans 108 (C9).
Du, J., Wu, Y., Huang, D., Zhang, J., 2010. Use of ^{7}Be, ^{210}Pb and ^{137}Cs tracers to the transport of surface sediments of the Changjiang Estuary, China. J. Mar. Syst. 82 (4), 286–294.
Emergency Operations Center, Ministry of Education, Culture, Sports, Science and Technology in Japan, 2011. Reading of environmental radioactivity level. http://www.mext.go.jp/english/incident/1303962.htm.
Evrard, O., Laceby, J.P., Lepage, H., Onda, Y., Cerdan, O., Ayrault, S., 2015. Radiocesium transfer from hillslopes to the Pacific Ocean after the Fukushima Nuclear Power Plant accident: a review. J. Environ. Radioact. 148, 92–110.
Garraffo, Z.D., Kim, H.C., Mehra, A., Spindler, T., Rivin, I., Tolman, H.L., 2016. Modeling of ^{137}Cs as a tracer in a regional model for the Western Pacific, after the Fukushima Daiichi Nuclear power plant accident of March 2011. Weather Forecast. 31 (2), 553–579.
Hirose, K., Sugimura, Y., Aoyama, M., 1992. Plutonium and ^{137}Cs in the western North Pacific: estimation of residence time of plutonium in surface waters. Int. J. Radiat. Appl. Instrum. Part A 43 (1–2), 349–359.
Hirose, K., Aoyama, M., Igarashi, Y., Komira, K., 2005. Extremely low background measurements of ^{137}Cs in seawater samples using an underground facility. J. Radioanal. Nucl. Chem. 263 (2), 349–353.
Hirose, K., Aoyama, M., Fukasawa, M., Kim, C.S., Komura, K., Povinec, P.P., Sanchez-Cabeza, J.A., 2007. Plutonium and ^{137}Cs in surface water of the South Pacific Ocean. Sci. Total Environ. 381 (1–3), 243–255.
Honda, M.C., Aono, T., Aoyama, M., Hamajima, Y., Kawakami, H., Kitamura, M., Masumoto, Y., Miyazawa, Y., Takigawa, M., Saino, T., 2012. Dispersion of artificial caesium-134 and -137 in the western North Pacific one month after the Fukushima accident. Geochem. J. 46, e1–d9.
Hu, Q.H., Weng, J.Q., Wang, J.S., 2010. Sources of anthropogenic radionuclides in the environment: a review. J. Environ. Radioact. 101 (6), 426–437.
Huang, D., Du, J., Moore, W.S., Zhang, J., 2013. Particle dynamics of the Changjiang Estuary and adjacent coastal region determined by natural particle-reactive radionuclides (^{7}Be, ^{210}Pb, and ^{234}Th). J. Geophys. Res.: Oceans. 118 (4), 1736–1748.
Inoue, M., Kofuji, H., Hamajima, Y., Nagao, S., Yoshida, K., Yamamoto, M., 2012. ^{134}Cs and ^{137}Cs activities in coastal seawater along Northern Sanriku and Tsugaru Strait, northeastern Japan, after Fukushima Dai-ichi Nuclear Power Plant accident. J. Environ. Radioact. 111, 116–119.
Ito, T., Aramaki, T., Kitamura, T., Otosaka, S., Suzuki, T., Togawa, O., Kobayashi, T., Senjyu, T., Chaykovskaya, E.L., Karasev, E.V., Lishavskaya, T.S., Novichkov, V.P., Tkalin, A.V., Shcherbinin, A.F., Volkov, Y.N., 2003. Anthropogenic radionuclides in the Japan Sea: their distributions and transport processes. J. Environ. Radioact. 68, 249–267.
Izrael, Y.A., 2007. Chernobyl radionuclide distribution and migration. Health Phys. 93 (5), 410–417.
Kim, C.K., Kim, C.S., Yun, J.Y., Kim, K.H., 1997. Distribution of ^{3}H, ^{137}Cs, and ^{239,240}Pu in the surface seawater around Korea. J. Radioanal. Nucl. Chem. 218 (1), 33–40.
Lee, H.J., Chao, S.Y., 2003. A climatological description of circulation in and around the East China Sea. Deep-Sea Res. II Top. Stud. Oceanogr. 50 (6), 1065–1084.
Lee, J.S., Takeshi, M., 2007. Intrusion of Kuroshio water onto the Continental Shelf of the East China Sea. J. Oceanogr. 63 (2), 309–325.
Lee, T.N., Johns, W.E., Liu, C.T., Zhang, D., Zantopp, R., Yang, Y., 2001. Mean transport and seasonal cycle of the Kuroshio east of Taiwan with comparison to the Florida Current. J. Geophys. Res. Oceans 106 (C10), 22143–22158.
Lie, H.J., Cho, C.H., 2002. Recent advances in understanding the circulation and hydrography of the East China Sea. Fish. Oceanogr. 11 (6), 318–328.
Liu, Z., Zheng, J., Pan, S., Dong, W., Yamada, M., Aono, T., Guo, Q., 2011. Pu and ^{137}Cs in the Yangtze River estuary sediments: distribution and source identification. Environ. Sci. Technol. 45, 1805–1811.
Liu, D., Hou, X., Du, J., Zhang, L., Zhou, W., 2016. ^{129}I and its species in the East China Sea: level, distribution, sources and tracing water masses exchange and movement. Sci. Rep. 6, 36611.
Matzko, J.R., 1994. Geology of the Chinese nuclear test site near Lop Nor, Xinjiang Uygur autonomous region, China. Eng. Geol. 36 (3–4), 173–181.
Miyao, T., Hirose, K., Aoyama, M., Igarashi, Y., 2000. Trace of the recent deep water

information in the Japan Sea deduced from historical ^{137}Cs data. Geophys. Res. Lett. 27 (22), 3731–3734.
Miyazawa, Y., Zhang, R., Guo, X., Tamura, H., Ambe, D., Lee, J.S., Okuno, A., Yoshinari, H., Setou, T., Komatsu, K., 2009. Water mass variability in the western North Pacific detected in a 15-year eddy resolving ocean reanalysis. J. Oceanogr. 65 (6), 737–756.
Nagaya, Y., Nakamura, K., 1992. ^{234,240}Pu and ^{137}Cs in the East China and the Yellow Seas. J. Oceanogr. 48, 23–35.
Povinec, P.P., Livingston, H.D., Shima, S., Aoyama, M., Gastaud, J., Goroncy, I., Hirose, K., Huynh-Ngoc, L., Ikeuchi, Y., Ito, T., Rosa, J.L., Kwong, L.L.W., Lee, S.H., Moriya, H., Mulsow, S., Oregioni, B., Pettersson, H., Togawa, O., 2003. IAEA'97 expedition to the NW Pacific Ocean—results of oceanographic and radionuclide investigations of the water column. Deep-Sea Res. II Top. Stud. Oceanogr. 50 (17), 2607–2637.
Povinec, P.P., Aarkrog, A., Buesseler, K.O., Delfanti, R., Hirose, K., Hong, G.H., Ito, T., Livingston, H.D., Nies, H., Noshkin, V.E., Shima, S., Togawa, O., 2005. ^{90}Sr, ^{137}Cs and ^{239,240}Pu concentration surface water time series in the Pacific and Indian Oceans–WOMARS results. J. Environ. Radioact. 81 (1), 63–87.
Povinec, P.P., Aoyama, M., Fukasawa, M., Hirose, K., Komura, K., Sanchez-Cabeza, J.A., Gastaud, J., Ješkovský, M., Levy, I., Sýkora, I., 2011. ^{137}Cs water profiles in the South Indian Ocean-an evidence for accumulation of pollutants in the subtropical gyre. Prog. Oceanogr. 89 (1–4), 17–30.
Povinec, P.P., Aoyama, M., Biddulph, D., Breier, R., Buesseler, K., Chang, C.C., Golser, R., Hou, X.L., Jeskovsky, M., Jull, A.J.T., Kaizer, J., Nakano, M., Nies, H., Palcsu, L., Papp, L., Pham, M.L., Steier, P., Zhang, L., 2013. Cesium, iodine and tritium in NW Pacific waters-a comparison of the Fukushima impact with global fallout. Biogeosciences 10, 5481–5496.
Qi, J., Yin, B., Zhang, Q., Yang, D., Xu, Z., 2014. Analysis of seasonal variation of water masses in East China Sea. Chin. J. Oceanol. Limnol. 32 (4), 958–971.
Sholkovitz, E.R., 1983. The geochemistry of plutonium in fresh and marine water environments. Earth Sci. Rev. 19 (2), 95–161.
Smith, J.N., Ellis, K.M., Kilius, L.R., 1998. ^{129}I and ^{137}Cs tracer measurements in the Arctic Ocean. Deep-Sea Res. I Oceanogr. Res. Pap. 45 (6), 959–984.
Smith, J.N., Brown, R.M., Williams, W.J., Robert, M., Nelson, R., Moran, S.B., 2015. Arrival of the Fukushima radioactivity plume in North American continental waters. Proc. Natl. Acad. Sci. 112 (5), 1310–1315.
Steinhauser, G., Brandl, A., Johnson, T.E., 2014. Comparison of the Chernobyl and Fukushima nuclear accidents: a review of the environmental impacts. Sci. Total Environ. 470–471, 800–817.
Stohl, A., Seibert, P., Wotawa, G., Arnold, D., Burkhart, J.F., Eckhardt, S., Tapia, C., Vargas, A., Yasunari, T.J., 2012. Xenon-133 and caesium-137 releases into the atmosphere from the Fukushima Dai-ichi nuclear power plant: determination of the source term, atmospheric dispersion, and deposition. Atmos. Chem. Phys. 12 (5), 2313–2343.
Su, J.L., 2001. A review of circulation dynamics of the coastal oceans near China. Acta Oceanol. Sin. 23 (4), 1–16.
Su, C.C., Huh, C.A., 2002. ^{210}Pb, ^{137}Cs and ^{239,240}Pu in East China Sea sediments: sources, pathways and budgets of sediments and radionuclides. Mar. Geol. 183 (1–4), 163–178.
Suzuki, T., Otosaka, S., Kuwabara, J., Kawamura, H., Kobayashi, T., 2013. Iodine-129 concentration in seawater near Fukushima before and after the accident at the Fukushima Daiichi Nuclear Power Plant. Biogeosciences 10 (6), 3839–3847.
Takano, K., 1991. Oceanography of Asian Marginal Seas. Elsevier Oceanography series, Tokyo, pp. 1–431.
Tumey, S.J., Guilderson, T.P., Brown, T.A., Broek, T., Buesseler, K.O., 2013. Input of ^{129}I into the western Pacific Ocean resulting from the Fukushima nuclear event. J. Radioanal. Nucl. Chem. 296 (2), 957–962.
UNSCEAR, 2008. Sources and effects of ionizing radiation (annex D). United Nations, New York.
Wang, J., Jiang, Y., Huang, D., Wen, T., Du, J., Zhang, J., 2012. Promotion of the lower limit of detection of gamma emitting nuclides in radioaerosol samples after Fukushima accident. J. Radioanal. Nucl. Chem. 292 (3), 1297–1301.
Wang, J., Du, J., Baskaran, M., Zhang, J., 2016. Mobile mud dynamics in the East China Sea elucidated using ^{210}Pb, ^{137}Cs, ^{7}Be and ^{234}Th as tracers. J. Geophys. Res. Oceans 121 (1), 224–239.
Wang, J., Baskaran, M., Niedermiller, J., 2017a. Mobility of ^{137}Cs in freshwater lakes: a mass balance and diffusion study of Lake St. Clair, Southeast Michigan, USA. Geochim. Cosmochim. Acta 218, 323–342.
Wang, J., Baskaran, M., Hou, X., Du, J.Z., Zhang, J., 2017b. Historical changes in ^{239}Pu and ^{240}Pu sources in sedimentary records in the East China Sea: implications for provenance and transportation. Earth Planet. Sci. Lett. 466, 32–42.
Wu, F., Zheng, J., Liao, H., Yamada, M., 2010. Vertical distributions of plutonium and ^{137}Cs in lacustrine sediments in northwestern China: quantifying sediment accumulation rates and source identifications. Environ. Sci. Technol. 44 (8), 2911–2917.
Wu, J., Zhou, K., Dai, M., 2013. Impacts of the Fukushima nuclearaccident on the China Seas: evaluation based on anthropogenic radionuclide ^{137}Cs. Chin. Sci. Bull. 58 (4–5), 552–558.
Yamada, M., Zheng, J., Wang, Z.L., 2006. ^{137}Cs, $^{239+240}$Pu and ^{240}Pu/^{239}Pu atom ratios in the surface waters of the western North Pacific Ocean, eastern Indian Ocean and their adjacent seas. Sci. Total Environ. 366 (1), 242–252.
Zhang, L., Liu, Z., Zhang, J., Hong, G., Park, Y., Zhang, H., 2007. Reevaluation of mixing among multiple water masses in the shelf: an example from the East China Sea. Cont. Shelf Res. 27, 1969–1979.